Rational design of thermostable vaccines by engineered peptide-induced virus self-biomineralization under physiological conditions

Guangchuan Wang[a,b], Rui-Yuan Cao[b], Rong Chen[c], Lijuan Mo[d], Jian-Feng Han[b], Xiaoyu Wang[b,e], Xurong Xu[e], Tao Jiang[b], Yong-Qiang Deng[b], Ke Lyu[c], Shun-Ya Zhu[b], E-De Qin[b], Ruikang Tang[a,e,1], and Cheng-Feng Qin[b,1]

[a]Center for Biomaterials and Biopathways, and [e]Qiushi Academy for Advanced Studies, Zhejiang University, Hangzhou 310027, China; [b]Department of Virology, State Key Laboratory of Pathogen and Biosecurity, Beijing Institute of Microbiology and Epidemiology, Beijing 100071, China; [c]Key Laboratory of Molecular Virology and Immunology, Institute Pasteur of Shanghai, Chinese Academy of Sciences, Shanghai 200025, China; and [d]Biomedical Center, Sir Run Run Shaw Hospital, Hangzhou 310016, China

The development of vaccines against infectious diseases represents one of the most important contributions to medical science. However, vaccine-preventable diseases still cause millions of deaths each year due to the thermal instability and poor efficacy of vaccines. Using the human enterovirus type 71 vaccine strain as a model, we suggest a combined, rational design approach to improve the thermostability and immunogenicity of live vaccines by self-biomineralization. The biomimetic nucleating peptides are rationally integrated onto the capsid of enterovirus type 71 by reverse genetics so that calcium phosphate mineralization can be biologically induced onto vaccine surfaces under physiological conditions, generating a mineral exterior. This engineered self-biomineralized virus was characterized in detail for its unique structural, virological, and chemical properties. Analogous to many exteriors, the mineral coating confers some new properties on enclosed vaccines. The self-biomineralized vaccine can be stored at 26 °C for more than 9 d and at 37 °C for approximately 1 wk. Both in vitro and in vivo experiments demonstrate that this engineered vaccine can be used efficiently after heat treatment or ambient temperature storage, which reduces the dependence on a cold chain. Such a combination of genetic technology and biomineralization provides an economic solution for current vaccination programs, especially in developing countries that lack expensive refrigeration infrastructures.

genetic engineering | vaccine design | shell

The development of vaccines against infectious diseases is one of the most successful medical interventions ever developed by humans (1, 2). Live attenuated viruses provide an effective vaccination strategy devised since the beginning of the vaccinology era, and vaccines against polio, smallpox, measles, rubella, yellow fever, Japanese encephalitis, and influenza, for example, have been used to immunize billions of children and adults worldwide. However, there are still more than 17 million deaths caused by infectious diseases every year, accounting for 25% of all deaths worldwide (3, 4). Most of the deaths are caused by vaccine-preventable diseases and the underutilization of vaccines. This is especially true for the poorest countries, because most vaccines are sensitive to heat and the cold chain is very difficult to maintain in countries with a minimal infrastructure. The poor efficacy and instability of vaccine products lead to incomplete immunization and a rapid loss of potency during storage and delivery, which severely limits the coverage of current vaccination programs. For example, ~50% of vaccine products are finally discarded due to poor thermostability (5). Refrigeration is essential for vaccines to maintain their quality. However, keeping vaccines at low temperatures is difficult and expensive. The cold chain consumes ~80% of the total cost of vaccination programs (3, 6), and it is not always reliable. The situation is even worse in developing countries and in the least-developed countries, where, due to the lack of extensive and reliable refrigeration infrastructure, over half of all deaths are caused by infectious diseases. Improving

the efficacy and thermostability of vaccines is of great importance and has been highlighted as a Grand Challenge in Global Health by the Gates Foundation (www.grandchallenges.org).

New advances in genetic and materials sciences have created the possibility of improving and stabilizing vaccine products. Stabilizers, such as deuterium oxide, proteins, $MgCl_2$, and non-reducing sugars, have been introduced to produce stabilized formulations of vaccines (7–9). By using reverse genetic technology, the viral capsid can be rationally engineered to improve its physicochemical properties (10–12). In nature, biomineralization is adopted by many organisms to improve their performance in harsh environments. For example, living organisms, such as diatoms (13), mollusks (14), eggs, and some plants (15), have developed biomineral exteriors that play a protective role. It should be noted that egg cells with mineral shells are extremely thermostable and can be stored under ambient conditions. Unfortunately, most living organisms, including vaccines, cannot generate such mineral shells due to the lack of biomineralization-related proteins, which usually play a key role in the control of biomineralization. Among biogenic minerals, calcium phosphate (CaP), the major component of bones and teeth, is of interest because of its unique biocompatibility (16), and it is now used as a transfer agent and adjuvant (17). CaP represents an excellent mineral shell candidate to stabilize vaccines. Recently, we have shown that a protective CaP shell can be introduced onto some virus surfaces in the presence of a high concentration of calcium ions (18, 19). However, the biomineralization process requires specific treatments and only occurs with selected premade viruses stocks. A natural virus cannot induce biomineralization by itself during its normal life cycle. In contrast, biomineralization in organisms is generally controlled using biomacromolecules in a mild biological system, and some polypeptides and macromolecules have been used to induce biomineralization (20–24). For example, several peptides have been genetically incorporated into the M13 bacteriophage and plant viruses as nucleators to direct nanomaterial synthesis (25, 26) or as specific nucleators for CaP mineralization in living systems (23, 27–29). Inspired by this achievement, we propose to design rationally an engineered virus carrying the selected biomimetic peptides that control the biomineralization process.

Human enterovirus type 71 (EV71) is a typical nonenveloped icosahedral virus belonging to the Picornaviridae family (30).

Picornaviruses cause acute diseases in humans and animals, including polio, hepatitis A, and foot-and-mouth disease. Live attenuated picornavirus vaccines are widely used with high efficacy. In this study, we protected the EV71 vaccine strain with an eggshell-like exterior, which is spontaneously formed under physiological conditions due to the engineered CaP biomineralization peptide. The biomineralized engineered vaccine exhibits overall improved thermostability and immunogenicity, and it can be used efficiently even after a week's storage at room temperature. Thus, "vaccines that can be stable in your pocket for 1 wk" can be created by the genetically induced self-biomineralization of the vaccine.

Results

Genetic Engineering. To endow a virus with the capacity of self-biomineralization, we aimed to display nucleating peptides on the virion surface to enhance its capacity to initiate CaP mineralization. Among nucleating peptides, two types of representative nucleators, a phosphate chelating agent (N6p) or calcium chelating agents (NWp and W6p), were selected. N6p is a reported CaP-binding peptide identified through phage display, and its binding effect is thought to be due to phosphate-chelating domains (SVKRGTSVG and VGMKPSP) (31). NWp is derived from the N-terminal 15-residue fragment of salivary statherin, a CaP high-affinity protein, and it has been used in biomimetic mineralization (32). W6p is an acidic analog of the amino-terminal 15-residue fragment of salivary statherin and core motifs of dentin matrix protein 1, an acidic protein that can trigger CaP formation in vitro by binding calcium ions (33). The site between amino acids 100 and 101 of the β-(BC)-loop of viral protein 1 (VP1) (Fig. 1A) has been demonstrated to be an appropriate insertion site for the placement of an engineered peptide on the viral surface (34, 35). The coding nucleotides of the above-mentioned nucleating peptides (Fig. 1A) were cloned into the infectious full-length cDNA of the attenuated EV71 strain A12 using standard DNA recombination technology (36). The engineered viruses carrying nucleating peptides were recovered by transfecting in vitro-transcribed RNAs into human rhabdomyosarcoma (RD) cells, and they were named EV71-N6, EV71-NW, and EV71-W6. DNA sequencing and indirect fluorescence assay (IFA) results (Figs. S1 and S2) confirmed that the nucleating peptides were successfully engineered into the viral genome. These genetically modified viruses exhibited similar growth patterns to the parental EV71 (Fig. 1B) and formed similar small plaques in RD cells (Fig. 1C), indicating that the incorporated peptides did not change viral replication. Structural modeling using the Phyre2 (Protein Homology/Analogy Recognition Engine 2) server showed that the insert peptide protruded from the natural VP1 proteins, and 60 copies of the nucleating peptides were predicted to be uniformly displayed on the surface of EV71 without affecting the original structure of the EV71 virion (Fig. 1D).

Self-Biomineralization. The engineered viral vaccines were incubated in calcium-enriched DMEM (calcium concentration of 5.5 mM) to evaluate their biomineralization capacity. Usually, viral particles can only be concentrated by ultracentrifugation under complicated conditions. When the viral particles were mineralized, they could be readily separated and concentrated by normal-speed centrifugation (18,000 × g for 10 min) due to the high relative gravity of the attached mineral phase. Thus, the biomineralization efficacy could be estimated by the ratio of viral particles in the supernatant and precipitate using plaque assays or quantitative RT-PCR (qRT-PCR) assays. For native EV71, few infectious viral particles were precipitated and most virions remained in the supernatant. As expected, native EV71 could not induce effective biomineralization (Fig. 2A). There was no significant difference between EV71 and EV71-N6, meaning that the integrated N6p peptide failed to induce vaccine biomineralization. However, the engineered EV71-NW and EV71-W6 viruses demonstrated enhanced biomineralization capacity. For EV71-W6, over 90% of infectious virions could be separated by centrifugation due to mineral incorporation (Fig. 2A). Dot blot
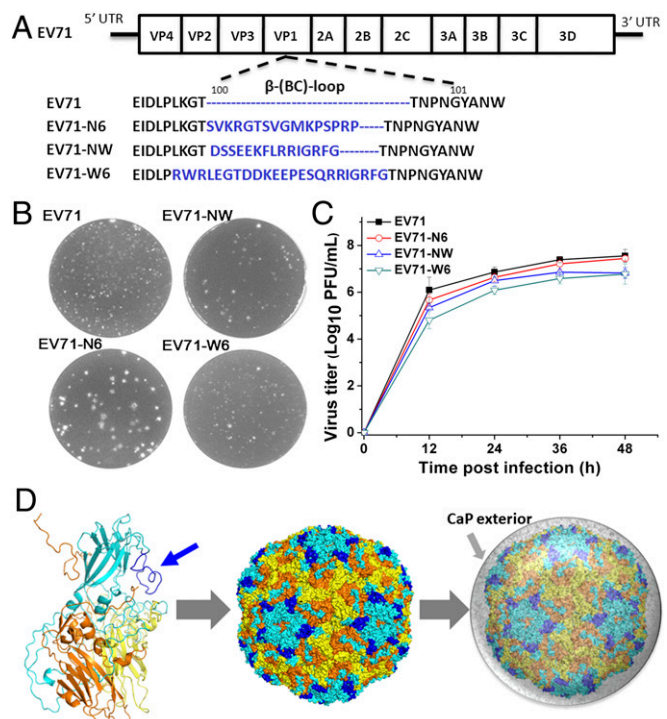

Fig. 1. Design and characterization of engineered EV71 carrying nucleating peptides. (A) EV71 genome and the insertion site of the β-(BC)-loop of VP1. (B) Plaque morphologies of parental EV71 and engineered viruses in RD cells. (C) One-step growth curves of parental EV71 and engineered viruses in RD cells [multiplicity of infection (MOI) = 0.1]. (D) Homology modeling of the mutant viral protein. EV71 capsid proteins VP1, VP2, and VP3 are shown in cyan, yellow, and orange, respectively. The inserted peptides are marked with blue, and 60 copies are uniformly distributed on the surface of the engineered EV71 virion. These peptides may induce in situ biomineralization to form a CaP mineral exterior (gray) for the vaccine.

assays revealed that the biomineralized EV71-W6 could barely be detected using EV71-specific antibodies. This experimental result implied that the capsid proteins were shielded by the precipitated mineral phase. In contrast, only some EV71-NW proteins and negligible quantities of EV71-N6 proteins were shielded by minerals due to their insufficient biomineralization (Fig. 2A, Upper).

SEM (Fig. 2B) and transmission EM (Fig. 2C) revealed that biomineralized EV71-W6 had a diameter of ~40 nm. The core-shell structure of the biomineralized vaccine was confirmed: The particle core was a 30-nm negatively stained (by phosphotungstic acid) virion (Fig. 2C, Inset), and it was surrounded by a 5- to 10-nm inorganic layer. Energy dispersive X-ray spectroscopy showed that the inorganic layer was CaP (Fig. 2B, Inset), and X-ray diffraction indicated that the mineral phase was amorphous (Fig. S3). The biomineralized EV71-W6 with the amorphous CaP coating was called EV71-W6-CaP. Importantly, the mineral exterior was stable at physiological pH > 7.0 but could be dissolved rapidly at pH < 6.5 (Fig. S4A). The release of the enclosed vaccine from the mineral coating was also demonstrated by dot blot assays in acidic solutions (Fig. S4B). This pH-sensitive feature is ideal for biomedical applications because slightly acidic conditions are frequently involved in the intracellular processing of internalized particles. We hypothesized that the mineral shell would not influence the vaccine's antigenicity, which was demonstrated by our following in vitro and in vivo assessments.

It should be emphasized that the serial passage of EV71-W6 in RD cells did not cause any loss of the W6p coding sequence. In our experiment, the coding sequence of W6p was still genetically stable after passaging 10 times, according to the sequencing
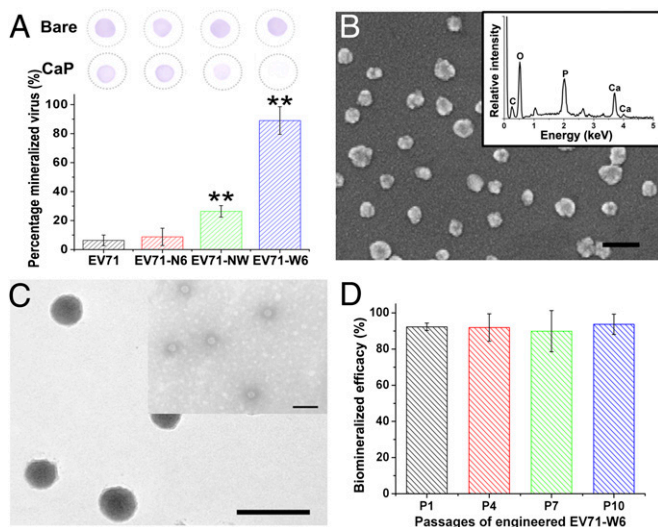
Fig. 2. Self-biomineralization of genetically engineered vaccines. (*A, Upper*) After biomineralization, the viral surface proteins were immunologically detected by dot blot assays to indicate the stealth conditions by the CaP exterior. (*A, Lower*) Following spontaneous mineralization and centrifugation, the biomineralization efficacy was determined by examining the infectious viral particles in the supernatant and pellet using plaque assays; error bars represent SDs ($n \geq 4$, Student's paired t test, one-tailed, $**P < 0.01$). (*B*) SEM images of CaP-mineralized EV71-W6; the inserted energy dispersive X-ray spectroscopy shows the presence of Ca and P on the vaccine surfaces. (Scale bar: 100 nm.) (*C*) Transmission EM images of biomineralized EV71-W6. (*Inset*) Image shows that each particle contains a negatively stained vaccine. (Scale bar: 100 nm.) (*D*) Biomineralization capacity of progeny EV71-W6 was determined by quantifying viral RNA using qRT-PCR assays; error bars represent SDs ($n \geq 3$).

results of the viral genome ([Fig. S2](#)), and the progeny EV71-W6 virus could still be efficiently self-biomineralized (Fig. 2*D*). Thus, self-biomineralization became an inheritable trait of EV71-W6, and future generations retained the inheritable CaP shell, which was attributed to the combination of genetic engineering and biomineralization.

Enhanced Immunogenicity. EV71-W6-CaP and EV71 caused similar cytopathic effects and plaque morphologies (Fig. 3*A*) in RD cells. One-step growth curves revealed similar growth patterns. The titer of EV71-W6-CaP was slightly higher than that of EV71-W6 at 12 h postinfection ([Fig. S5](#)). The results from IFA with EV71-specific antibodies showed that EV71-W6-CaP was infectious; the viral antigens were expressed as in EV71-W6 and parental EV71 (Fig. 3*B*, green), and the cell nucleus was stained by DAPI (Fig. 3*B*, blue). The expression of viral antigens was higher after CaP mineralization at the early stage in RD cells (Fig. 3*B*). Such infection enhancement was more obvious in Vero cells (approximately onefold higher) and THP-1 cells (greater than twofold higher). Furthermore, the biomineralization treatment did not enhance virulence in animals, and EV71-W6-CaP remained nonvirulent to suckling mice. These results revealed that CaP biomineralization did not alter either viability or the original attenuation of virus. It follows that a biomineralized vaccine could be used directly in biomedical applications.

The immunogenicity of the biomineralized vaccine was also evaluated in vivo. The results revealed that at 4 wk postimmunization, EV71-W6-CaP induced ~3.5-fold higher serum IgG (Fig. 3*C*) and almost twofold higher neutralization antibody titers (Fig. 3*D*) in mice than native EV71 did. EV71-W6 induced similar levels of IgG and neutralizing antibodies as EV71. The results indicated that it is the biomineralized CaP exterior, rather than the genetic engineering itself, that contributed to the

immunogenicity enhancement of vaccines. Nevertheless, the CaP shell formation was induced by the integrated W6p.

Improved Thermostability. EV71-W6-CaP, EV71-W6, and parental EV71 were incubated at room temperature (26 °C) for varying numbers of days, and their subsequent infectivities were titrated by plaque assays. These data are represented in a logarithmic scale as a function of the storage time. EV71-W6 and parental EV71 shared similar thermal inactivation kinetics, with inactivation rate constants of 0.25246 d^{-1} and 0.26011 d^{-1}, respectively (Fig. 4*A*). They exhibited ~1-$\log_{10}$ plaque-forming unit (PFU; 90%), 2-$\log_{10}$ PFU (99%), and 4-$\log_{10}$ PFU (99.99%) losses after 3, 6, and 14 d of storage, respectively. According to indices of the World Health Organization requirement for vaccine efficacy (37), no more than a 1-$\log_{10}$ reduction of the initial titer is permitted. Therefore, the room temperature storage of EV71 or EV71-W6 should be less than 3 d, and the genetic engineering alone did not alter viral thermostability in our case. After the combination of self-biomineralization, the resulting EV71-W6-CaP exhibited a significantly slower inactivation rate (0.09921 d^{-1}) and its storage could be prolonged to more than 9 d at 26 °C. In tropical areas, ambient temperature is always >30 °C or even >40 °C, such that an examination of the vaccine storage period at high temperatures is also of importance. Accelerated degradation tests with samples subjected to physiological temperature (37 °C) and tropical zone temperature (42 °C) were performed to estimate vaccine potency loss. CaP mineralization reduced the inactivation kinetics of the engineered vaccine EV71-W6 nearly threefold, according to its inactivation rate constants (Fig. 4 *B* and *C*). At 37 °C, EV71-W6, similar to parental EV71, lost ~1 $\log_{10}$ PFU at 44 h, whereas EV71-W6-CaP lost only 1 $\log_{10}$ PFU at 168 h (Fig. 4*B*). At 42 °C, EV71-W6-CaP was viable even after storage for 9 h, whereas the storage times of EV71-W6 and parental EV71 should be less than 2.5 h (Fig. 4*C*). However, the same treatment could only improve the thermostability of native EV71 by less than 1.4-fold due to its poor biomineralization capacity ([Fig. S6](#)). These results indicated that CaP biomineralization greatly improved vaccine thermostability and the improvement was directly related to biomineralization efficacy.

The immunogenicity of the heat-treated vaccines was then verified in animals. All vaccines were incubated at 37 °C for 5 d, and groups of BALB/c mice were then s.c. immunized. EV71-W6-CaP induced a similar amount of neutralization antibodies after storage, whereas a significant (~75%) decrease in EV71-specific IgG titers (Fig. 5*A*) and a more than 50% decrease in neutralization antibody titers (Fig. 5*B*) were observed for native viruses after storage. Additionally, the capacity to elicit a cellular response was determined. Because the frequencies of IFN-γ–secreting cells were commonly examined to determine the T-cell response, the levels of EV71-specific IFN-γ–secreting splenocytes induced by native and biomineralized vaccines were determined by enzyme-linked immunospot assays. The stored EV71-W6-CaP could induce high frequencies of EV71-specific IFN-γ–secreting cells in mice, and no significant decrease was observed compared with the fresh virus without storage (Fig. 5*C*). However, the same storage resulted in a significant ~40% decrease in the frequencies of EV71-specific IFN-γ–secreting cells induced by nonbiomineralized EV71-W6 and parental EV71 (Fig. 5*C*). Collectively, the genetically induced biomineral shell significantly improved the thermostability of the vaccine to the point that it could be viable for use in a vaccine program even after a week's storage at ambient temperatures without refrigeration. This new feature indicates that the engineered vaccines could be less dependent on the cold chain.

Discussion

By genetically engineering potential nucleating peptides onto the surfaces of live viruses, we rationally designed a self-biomineralized virus with improved thermostability and immunogenicity. This CaP biomineralization capacity was given to EV71-W6 by genetically engineering a CaP nucleating peptide onto the viral
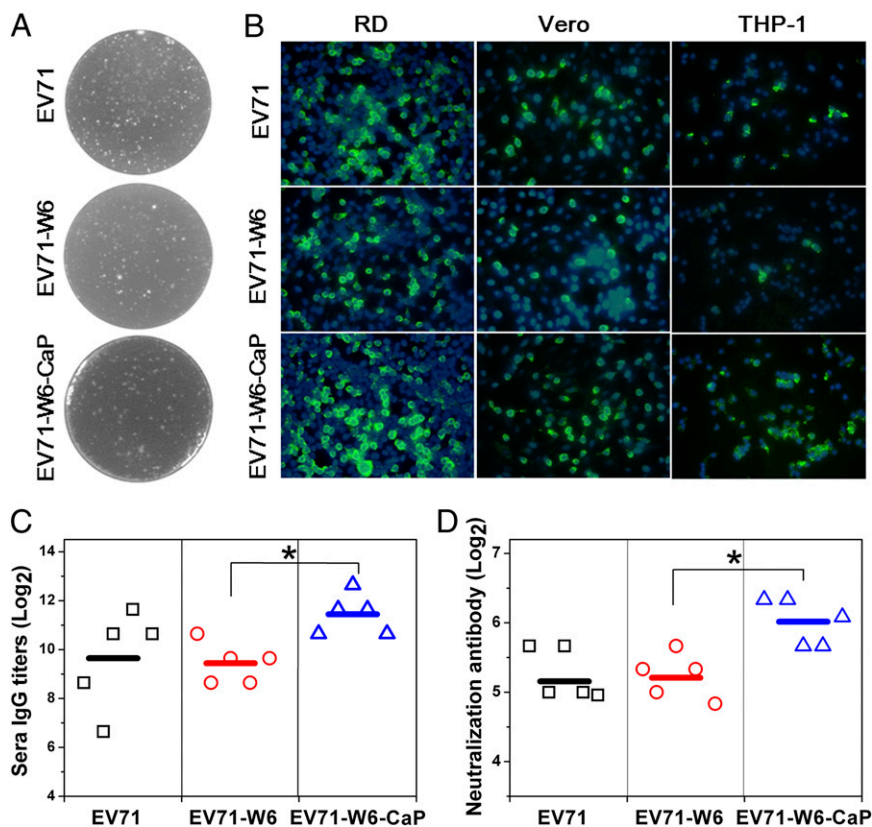
Fig. 3. Biological characterizations. (*A*) Plaque morphologies of EV71, EV71-W6, and EV71-W6-CaP in RD cells. (*B*) Indirect immunological fluorescence of recovered virus in Vero cells, RD cells (MOI = 0.1), and THP-1 cells (MOI = 1) at 12 h postinfection; the cell nuclei were stained by DAPI (blue). (Magnification: *B*, 40×.) (*C*) EV71-specific serum IgG titers of mice ($n \geq 5$) at 4 wk postimmunization. (*D*) Serum neutralization antibody titers of mice ($n \geq 5$) at 4 wk post-immunization were determined by micro-neutralization assays (Student's paired *t* test, one-tailed, *$P < 0.05$).

capsid. Sixty copies of the engineered peptide provide CaP nucleation sites on the vaccine surface because they can concentrate calcium ions from incubation solutions, increasing CaP supersaturation around the vaccine and leading to localized mineralization. In this study, EV71-W6 and EV71-NW displayed improved CaP biomineralization capacity, whereas EV71-N6 did not exhibit significantly increased biomineralization. This result indicates that cationic calcium ion-chelating peptide motifs, rather than phosphate ion-chelating motifs, can efficiently initiate CaP mineralization, which is also in accordance with the previous understanding that anionic peptides are more effective in eliciting CaP biomineral generation (23, 33, 38, 39). That EV71-W6 displayed better self-biomineralization capacity than EV71-NW may due to the higher density of anionic Glu and Asp amino acids in W6p. It has been documented that Glu and Asp are the most active residues for inducing biomineralization in

nature (40, 41). In comparison to W6p, NWp cannot initiate CaP mineralization efficiently because the Ser residues in NWp are replaced by Asp and Glu in W6p. The abundant Asp and Glu residues make W6p more active in CaP mineralization. This phenomenon reveals the relationship between biomimetic peptides and biomineralization controls. We conclude that the biomineralization capacity of living organisms can be regulated by the genetic engineering of nucleating peptides. Again, our study confirms the importance of Glu and Asp residues in CaP biomineralization proteins. Compared with our previous work on the biomineralization of purified adenovirus by incubation with calcium ions and phosphate titration and the biomineralization of enveloped viruses in a high-calcium environment, this genetic strategy confers to the virus an automatic self-biomineralization capacity under physiological conditions, which benefits uniform formation of a reliable mineral exterior.
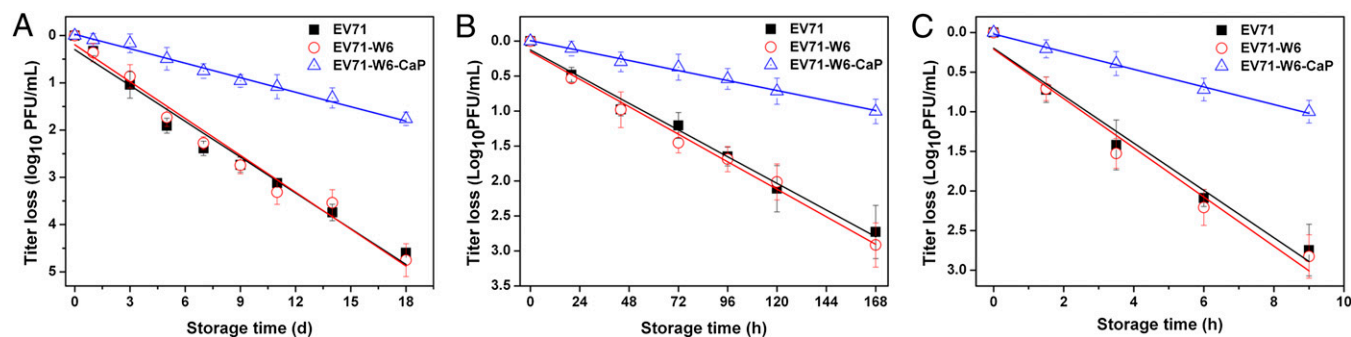

Fig. 4. In vitro tests of virus thermostability. Thermal-inactivation kinetics were determined at 26 °C (*A*), 37 °C (*B*), or 42 °C (*C*). The remaining percentage of infectivity is represented in a logarithmic scale as a function of incubation time ($n \geq 4$); error bars represent SDs. The calculated average inactivation rate constants for EV71, EV71-W6, and EV71-W6-CaP, as shown in the figures, were $K_{EV71} = 0.25246$ d^{-1}, $K_{EV71-W6} = 0.26011$ d^{-1}, and $K_{EV71-W6-CaP} = 0.09921$ d^{-1} at 26 °C; $K_{EV71} = 0.01590$ h^{-1}, $K_{EV71-W6} = 0.01639$ h^{-1}, and $K_{EV71-W6-CaP} = 0.00594$ h^{-1} at 37 °C; and $K_{EV71} = 0.29896$ h^{-1}, $K_{EV71-W6} = 0.31073$ h^{-1}, and $K_{EV71-W6-CaP} = 0.11117$ h^{-1} at 42 °C.
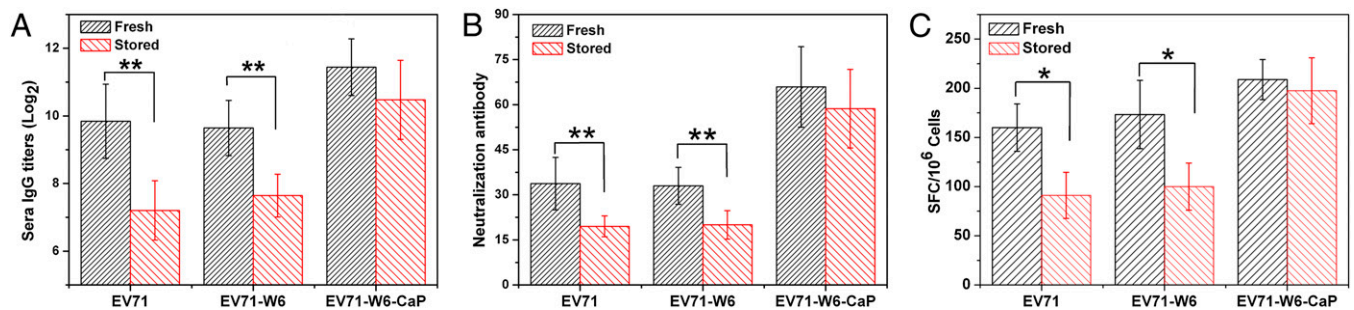
Fig. 5. Animal tests of stored vaccines. EV71-specific IgG titers (*A*) and neutralizing antibody responses induced in mice by EV71, EV71-W6, and EV71-W6-CaP after 5 d of storage at 37 °C (*B*). Antibody titers were determined at 4 wk postimmunization ($n \geq 5$); error bars represent SDs. (*C*) Frequencies of EV71-specific INF-γ–secreting splenocytes in the immunized mice before and after storage. Splenocytes were isolated from the immunized mice at 2 wk postimmunization and subjected to enzyme-linked immunospot assay ($n \geq 3$); error bars represent SDs (Student's paired *t* test, one-tailed, *P < 0.05, **P < 0.01). SFC, spot forming cells.

The spontaneous release of the enclosed vaccine from the mineral shell is key to ensure the availability of biomineralized vaccine. The CaP biomineral phase exhibits its advantage in protection and release due to its pH-dependent stability. It has been found that the mineral exterior is stable under extracellular conditions, because the pH of body fluids is ~7.4 (42). However, when the biomineralized vaccine is taken up by cells, the internalization process is often accompanied by acidic conditions, such as endosomes, which can induce the spontaneous degradation of the CaP exterior. After biomineralization, the CaP shell will not hinder the infectivity of vaccines, and the biomineralized virus shares similar replication and growth patterns with the native virus (Fig. 3*A* and Fig. S5). The entry of the biomineralized virus into host cells may be more like the noninfectious virus-like particles that have differential uptake by dendritic cells and other antigen-presenting cells. Our results reveal that higher virus titers and viral protein expression are observed in EV71-W6-CaP–infected cells at the early stage of infection, and the enhancement of infectivity is more obvious in viral receptor-deficient cells (Fig. 3*B*), which is in accord with our previous findings (19). This infectivity enhancement is restricted to the primary infection when the virus possesses mineral shells; therefore, it may favor the efficacy of vaccines without elevating their virulence. Additionally, because the CaP exterior can shelter the vaccine and help the vaccine escape direct clearance, the eliciting of IFN-α and IFN-β in EV71-W6-CaP–infected cells is delayed (Fig. S7).

The vaccine with a protective shell, EV71-W6-CaP, exhibits an ideal thermostability, extending its storage time by nearly threefold. It can be understood by means of the isolation of enclosed vaccine from destructive external adverse factors by means of the spontaneously biomineralized CaP exterior, which may protect viral proteins from thermal inactivation by insulating the direct interactions between water solutions and vaccines (14). Furthermore, an attachment of the mineral phase can stabilize the protein and subunit structures on vaccine surfaces by means of the direct binding effect between CaP and biomineralization peptide. If the immunogenicity enhancement conferred by this CaP biomineralization is taken into consideration, the total efficacy of the vaccine can be significantly improved by this modification. The self-biomineralized vaccines exhibit higher efficacies in vivo even after storage at ambient temperatures, which simplifies their application.

Developing regions lacking extensive, reliable refrigeration infrastructures are particularly vulnerable to vaccine failure, which, in turn, increases the burden of disease. It is estimated that at least 3 million children die of infectious diseases that are preventable with presently available but underused vaccines, and the death toll of vaccine-preventable meningitis, pneumonia, and diarrheal disease remains a major cause of death in Africa (4). Therefore, the maintenance of vaccine efficacy without a cold chain has the potential to extend immunity against deadly diseases to the world's poorest communities. Development of a robust vaccine is promising for a wide variety of vaccines. Inspired by nature, we engineered nucleating peptides into vaccines by reverse genetics to produce self-biomineralized vaccines with a mineral exterior as a proof of concept. The exterior confers improved thermal stability and immunogenicity to the enclosed vaccine. Our results indicate that under a wide range of ambient temperatures, the biomineralized vaccine can be guaranteed for use in a health clinic without any access to refrigeration for at least 1 d, which is often the situation in clinics located in tropical climates with unreliable cold chains. Most reconstituted vaccines lose potency rapidly and must be used within a few hours (9, 37), and the vaccine exposure time out of the cold chain should be kept as short as possible. This achievement means that we may be able to create a thermostable vaccine in a liquid formulation without freeze-drying and reconstitution before injection. Furthermore, current immunization programs in resource-limited areas are greatly hampered by the terminal distribution of vaccines from local storage centers to immunization clinics or mobile on-site utilization. The biomineralized vaccine described in our study will no doubt gain additional exposure time. Also, temperature monitor studies have indicated that the deviation from ideal storage temperature is inevitable (43) and that occasional that cold chain breakdown cases occur. The enhanced thermostability of a vaccine is thereby supposed to reduce its validity loss during storage and transportation. Robust liquid vaccines produced with less dependence on cold chains can provide benefits by reducing waste, ensuring potency, and decreasing financial cost, which are highly helpful to expand the global coverage of vaccination programs (44, 45).

Unlike previous attempts, we combined biomimetic mineralization and genetic engineering to produce self-biomineralized vaccines, and the resulting vaccines have inheritable performance improvements. Such biomineralization capacity resulting from genetic engineering is inheritably stable, and our study shows that the mineralization efficacy and improved thermostability can be maintained after serial passages. Vaccine biomineralization can be spontaneously induced under biological conditions after genetic modification so that the improvement is costless, which allows pharmaceutical companies to manufacture thermostable vaccines economically. Furthermore, the strategy combines the advantages of genetic engineering and biomineralization, and it is easily reproduced. Currently, most viral protective antigens and virion structures have been resolved so that they can readily be genetically reconstructed. Furthermore, pseudovirus particles and other biological products can also be modified to display a specific nucleating peptide that will confer biomineralization capacity onto the product. In general, analogous improvement by genetically induced self-biomineralization can be used in more viral vaccines. This strategy may hold significant promise for vaccination programs by providing a feasible path toward large-scale thermostable vaccine production, with advantages that include being fast, inexpensive, and easily adapted to any other live vaccines. However, as with any other new technologies, the manufacturing process and safety profile should be carefully evaluated before the use of these thermostable vaccines in clinical practice.

Conclusions

We used a combination of genetic engineering and biomineralization techniques to produce a thermostable vaccine. The self-directed biomineralized vaccine can be used efficiently after storage at ordinary temperatures, which significantly increases the efficacy of immunization systems and lowers the cost of vaccine delivery and storage. We suggest that this simple attempt can be developed into a general strategy for vaccine improvement to assist in the execution and expansion of immunization programs globally, especially for the poorest countries.

Materials and Methods

More detailed descriptions of the experimental procedures and data analysis are provided in *SI Materials and Methods*.

Construction and Recovery of Recombinant Vaccines. The coding nucleotides of nucleating peptides N6p (SVKRGTSVGMKPSPRP), NWp (DSSEEKFLRRIGRFG), and W6p (RWRLEGTDDKEEPESQRRIGRFG) were cloned into the β-(BC)-loop of a full-length infectious cDNA clone of EV71-attenuated strain A12 using the fusion PCR technique as previously described (36). The recombinant plasmids carrying the biomimetic peptides were linearized and used as templates for in vitro transcription, which was performed using the Ribo-MAX Large Scale Production System (Promega) according to the manufacturer's protocols. The yield and integrity of transcripts were analyzed by gel electrophoresis under nondenaturing conditions. RNA transcripts (5 μg) were transfected with Lipofectamine 2000 (Invitrogen) into RD cells grown in 60-mm-diameter culture dishes. Supernatants were then harvested at ~3–5 d posttransfection, when typical cytopathic effects were observed. The supernatants were then clarified by low-speed centrifugation. All the plasmids mentioned above were confirmed by DNA sequencing.

Vaccine Biomineralization. Vaccine solutions (10^6–10^8 pfu/mL) in DMEM supplemented with 1–4 mM calcium chloride were incubated at 37 °C for 6 h. The biomineralized viruses were separated by centrifugation at $16,000 \times g$ for 10 min. The biomineralization efficacy was determined by measuring the percentage of viral RNA and infectious particles in the deposit by qRT-PCR and plaque assays, respectively. Calcium chloride, at 3.7 mM, was used as the optimized concentration throughout our experiments.

Animal Assessments. Animal experiments were approved by and performed in strict accordance with the guidelines of the Animal Experiment Committee of the State Key Laboratory of Pathogen and Biosecurity, Ministry of Science and Technology of the People's Republic of China. Groups of BALB/c mice were s.c. immunized with fresh or stored EV71, EV71-W6, or EV71-W6-CaP, respectively. Sera were collected at 14 and 28 d postinfection. All samples had the same initial titers before storage (200 μL, 10^6 pfu/mL). Serum IgG and neutralization antibodies were detected by ELISA and microneutralization assays, respectively.

1. Rappuoli R, Miller HI, Falkow S (2002) Medicine. The intangible value of vaccination. *Science* 297(5583):937–939.
2. Rappuoli R, Mandl CW, Black S, De Gregorio E (2011) Vaccines for the twenty-first century society. *Nat Rev Immunol* 11(12):865–872.
3. Chen X, et al. (2011) Improving the reach of vaccines to low-resource regions, with a needle-free vaccine delivery device and long-term thermostabilization. *J Control Release* 152(3):349–355.
4. Clemens J, Holmgren J, Kaufmann SH, Mantovani A (2010) Ten years of the Global Alliance for Vaccines and Immunization: Challenges and progress. *Nat Immunol* 11(12):1069–1072.
5. Schlehuber LD, et al. (2011) Towards ambient temperature-stable vaccines: The identification of thermally stabilizing liquid formulations for measles virus using an innovative high-throughput infectivity assay. *Vaccine* 29(31):5031–5039.
6. Das P (2004) Revolutionary vaccine technology breaks the cold chain. *Lancet Infect Dis* 4(12):719.
7. Milstien JB, Lemon SM, Wright PF (1997) Development of a more thermostable poliovirus vaccine. *J Infect Dis* 175(Suppl 1):S247–S253.
8. Alcock R, et al. (2010) Long-term thermostabilization of live poxviral and adenoviral vaccine vectors at supraphysiological temperatures in carbohydrate glass. *Sci Transl Med* 2(19):19ra12.
9. Zhang H, et al. (2012) Stabilization of vaccines and antibiotics in silk and eliminating the cold chain. *Proc Natl Acad Sci USA* 109(30):11981–11986.
10. Mateu MG (2011) Virus engineering: Functionalization and stabilization. *Protein Eng Des Sel* 24(1-2):53–63.
11. Reguera J, Carreira A, Riolobos L, Almendral JM, Mateu MG (2004) Role of interfacial amino acid residues in assembly, stability, and conformation of a spherical virus capsid. *Proc Natl Acad Sci USA* 101(9):2724–2729.
12. Mateo R, Luna E, Rincón V, Mateu MG (2008) Engineering viable foot-and-mouth disease viruses with increased thermostability as a step in the development of improved vaccines. *J Virol* 82(24):12232–12240.
13. Hamm CE, et al. (2003) Architecture and material properties of diatom shells provide effective mechanical protection. *Nature* 421(6925):841–843.
14. Yao HM, et al. (2010) Protection mechanisms of the iron-plated armor of a deep-sea hydrothermal vent gastropod. *Proc Natl Acad Sci USA* 107(3):987–992.
15. Epstein E (2009) Silicon: Its manifold roles in plants. *Ann Appl Biol* 155(2):155–160.
16. Palmer LC, Newcomb CJ, Kaltz SR, Spoerke ED, Stupp SI (2008) Biomimetic systems for hydroxyapatite mineralization inspired by bone and enamel. *Chem Rev* 108(11):4754–4783.
17. He Q, et al. (2000) Calcium phosphate nanoparticle adjuvant. *Clin Diagn Lab Immunol* 7(6):899–903.
18. Wang G, et al. (2012) Eggshell-inspired biomineralization generates vaccines that do not require refrigeration. *Angew Chem Int Ed Engl* 51(42):10576–10579.
19. Wang X, et al. (2012) Biomineralization-based virus shell-engineering: Towards neutralization escape and tropism expansion. *Adv Healthc Mater* 1(4):443–449.
20. Prieto S, et al. (2011) Biomimetic calcium phosphate mineralization with multifunctional elastin-like recombinamers. *Biomacromolecules* 12(5):1480–1486.
21. Wong Po Foo C, et al. (2006) Novel nanocomposites from spider silk-silica fusion (chimeric) proteins. *Proc Natl Acad Sci USA* 103(25):9428–9433.
22. Wang E, Lee SH, Lee SW (2011) Elastin-like polypeptide based hydroxyapatite bionanocomposites. *Biomacromolecules* 12(3):672–680.
23. Hartgerink JD, Beniash E, Stupp SI (2001) Self-assembly and mineralization of peptide-amphiphile nanofibers. *Science* 294(5547):1684–1688.
24. Wang G, et al. (2010) Extracellular silica nanocoat confers thermotolerance on individual cells: A case study of material-based functionalization of living cells. *ChemBioChem* 11(17):2368–2373.
25. Lee YJ, et al. (2009) Fabricating genetically engineered high-power lithium-ion batteries using multiple virus genes. *Science* 324(5930):1051–1055.
26. Lee SY, Royston E, Culver JN, Harris MT (2005) Improved metal cluster deposition on a genetically engineered tobacco mosaic virus template. *Nanotechnology* 16(Suppl 7):435–441.
27. He G, George A (2004) Dentin matrix protein 1 immobilized on type I collagen fibrils facilitates apatite deposition in vitro. *J Biol Chem* 279(12):11649–11656.
28. Sarikaya M, Tamerler C, Jen AK, Schulten K, Baneyx F (2003) Molecular biomimetics: Nanotechnology through biology. *Nat Mater* 2(9):577–585.
29. Dickerson MB, Sandhage KH, Naik RR (2008) Protein- and peptide-directed syntheses of inorganic materials. *Chem Rev* 108(11):4935–4978.
30. Wang XX, et al. (2012) A sensor-adaptor mechanism for enterovirus uncoating from structures of EV71. *Nat Struct Mol Biol* 19(4):424–429.
31. Roy MD, Stanley SK, Amis EJ, Becker ML (2008) Identification of a highly specific hydroxyapatite-binding peptide using phage display. *Adv Mater* 20(10):610–617.
32. Holt C, Sørensen ES, Clegg RA (2009) Role of calcium phosphate nanoclusters in the control of calcification. *FEBS J* 276(8):2308–2323.
33. He G, Dahl T, Veis A, George A (2003) Nucleation of apatite crystals in vitro by self-assembled dentin matrix protein 1. *Nat Mater* 2(8):552–558.
34. Arita M, et al. (2007) An attenuated strain of enterovirus 71 belonging to genotype a showed a broad spectrum of antigenicity with attenuated neurovirulence in cynomolgus monkeys. *J Virol* 81(17):9386–9395.
35. Evans DJ, et al. (1989) An engineered poliovirus chimaera elicits broadly reactive HIV-1 neutralizing antibodies. *Nature* 339(6223):385–388, 340.
36. Kung YH, et al. (2010) Introduction of a strong temperature-sensitive phenotype into enterovirus 71 by altering an amino acid of virus 3D polymerase. *Virology* 396(1):1–9.
37. Galazka A, Milstien J, Zaffran M (1998) *Thermostability of Vaccines: Global Programme for Vaccines and Immunization (GPV)* (World Health Organization, Geneva).
38. Addadi L, Weiner S (1985) Interactions between acidic proteins and crystals: Stereochemical requirements in biomineralization. *Proc Natl Acad Sci USA* 82(12):4110–4114.
39. George A, Veis A (2008) Phosphorylated proteins and control over apatite nucleation, crystal growth, and inhibition. *Chem Rev* 108(11):4670–4693.
40. Chu X, et al. (2011) Unique roles of acidic amino acids in phase transformation of calcium phosphates. *J Phys Chem B* 115(5):1151–1157.
41. Tao J, Zhou D, Zhang Z, Xu X, Tang R (2009) Magnesium-aspartate-based crystallization switch inspired from shell molt of crustacean. *Proc Natl Acad Sci USA* 106(52):22096–22101.
42. Duprat F, et al. (1997) TASK, a human background K+ channel to sense external pH variations near physiological pH. *EMBO J* 16(17):5464–5471.
43. Braun LJ, et al. (2009) Characterization of a thermostable hepatitis B vaccine formulation. *Vaccine* 27(34):4609–4614.
44. Levin A, Levin C, Kristensen D, Matthias D (2007) An economic evaluation of thermostable vaccines in Cambodia, Ghana and Bangladesh. *Vaccine* 25(39-40):6945–6957.
45. Chen D, et al. (2010) Thermostable formulations of a hepatitis B vaccine and a meningitis A polysaccharide conjugate vaccine produced by a spray drying method. *Vaccine* 28(31):5093–5099.